Ex-situ Carbon Capture Storage (CCS) techniques and decomposition analysis for the reduction of CO_2 emission in the eco-industrial parks

Seok Jung[a*], Li Pang Wang[a], Gjergj Dodbiba[a], Kyoung-Jin An[b], Toyohisa Fujita[a]

[a] Department of Systems Innovation, Graduate School of Engineering, The University of Tokyo, Eng. Bldg. 4, Room 131, 7-3-1 Hongo, Bunkyo-Ku, Tokyo 113-8656, Japan
[b] Department of Urban Engineering, Graduate School of Engineering, The University of Tokyo, Eng. Bldg. 14, Room 815, 7-3-1 Hongo, Bunkyo-Ku, Tokyo 113-8656, Japan

Abstract

Carbon dioxide (CO_2) emissions are a leading contributor to the negative effects of global warming. Globally, research has focused on effective means of reducing and mitigating CO_2 emissions. In this study, we examined the efficacy of eco-industrial parks (EIPs) and accelerated mineral carbonation techniques in reducing CO_2 emissions in South Korea. First, we used Logarithmic Mean Divisia Index (LMDI) analysis to determine the trends in carbon production and mitigation at the existing EIPs. We found that, although CO_2 was generated as byproducts and wastes of production at these EIPs, improved energy intensity effects occurred at all EIPs, and we strongly believe that EIPs are a strong alternative to traditional industrial complexes for reducing net carbon emissions. We also examined the optimal conditions for using accelerated mineral carbonation to dispose of hazardous fly ash produced through the incineration of municipal solid wastes at these EIPs. We determined that this technique most efficiently sequestered CO_2 when micro-bubbling, low flow rate inlet gas, and ammonia additives were employed.

Keywords: CO_2 emissions, LMDI analysis, Accelerated mineral carbonation, EIPs

	Nomenclature		
C_{tot}	Carbon emission	M_{ij}	EC_{ij}/TEC_i
C_{pdn}	Production effect	I_i	$TEC_i/GRDP_i$
C_{int}	Energy intensity effect	G_i	$GRDP_i/P_i$
C_{mix}	Fuel mix effect	P_i	Population size
C_{emf}	Emission effect	i	Year
C_{pop}	Population effect	j	Fuel type
P	Population	α_1	First step carbonated weight
GRDP	Gross regional domestic product	β	Carbonated raw material weight
TEC	Total energy consumption	α_2	Second step carbonated weight
EC	Fossil fuel energy consumption	γ	CO_2 conversion volume to $CaCO_3$
E_{ij}	CO_{2ij}/EC_{ij}		

Introduction

Rapid urbanization and anthropogenic disturbance have resulted in various environmental challenges. One major challenge is the threat of global climate change, intensified by the release of greenhouse gases (GHGs) generated as wastes and byproducts of anthropogenic activities such as the large-scale burning of fossil fuels. Global climate change is predicted to have drastic, negative impacts on natural meteorological patterns and ecosystem functioning as well as on human economic activities (IPCC, 2007).

Carbon dioxide (CO_2), produced primarily through fossil fuel consumption and urbanization, is one GHG known to be a main contributor of global climate change, resulting in an increase in the average surface temperature of the Earth since the beginning of the Industrial Revolution (IPCC, 2007).

As a result of international cooperative agreements like the Kyoto Protocol outlined by the United Nations Framework Convention on Climate Change, many countries have adopted policies aimed at reducing CO_2 emissions; the European Union plans to reduce

GHGs to 20% of 1990 levels while the USA and Japan have pledged to reduce levels to 17% and 15%, respectively, of 2005 levels by 2020 (PCGG, 2009). In addition, countries not considered as one of the 37 Annex I countries under the Kyoto Protocol have also pledged to reduce CO_2 emissions. For example, South Korea, which is the 9th largest producer of GHGs in the world (IEA, 2011), plans to reduce GHGs to 30% of the business as usual (BAU) level by 2020 and to focus on environmentally-friendly industrial development strategies under a slogan of 'Low Carbon, Green Growth' (PCGG, 2009).

In accordance with the seriousness of the threat of GHGs to the environment, a great deal of research has focused on factors influencing CO_2 emissions and on the development of strategies used to mitigate those emissions. One strategy currently being employed in South Korea is the use of eco-industrial parks (EIPs), defined by the United States President's Council on Sustainable Development (PCSD) as 'a community of businesses that cooperate with each other and with the local community to efficiently share resources (information, materials, water, energy, infrastructure and natural habitat), leading to economic and environmental quality gains, and equitable enhancement of human resources for the business and local community' (PCSD, 1996). Under the EIP concept, various techniques are employed to efficiently use space and resources while minimizing the production of waste products. The EIP initiative has been attempted as a way to reduce carbon dioxide emissions by both developing and developed countries worldwide, including Europe (Baas and Boons, 2004; Tudor et al., 2007), China (Fang et al., 2007; Zhang et al., 2010), USA (Gibbs and Deutz, 2005, 2007), Australia (Roberts, 2004), and Japan (Berkel et al., 2009). In South Korea, existing industrial complexes, which have played pivotal roles in economic growth since the 1960s, are being converted into EIPs. Industrial complexes historically served as export outposts, magnets for large-scale installation industries, and as a means of fostering

growth in rural areas (KICOX, 2008). However, with continuing urbanization and the downturn of the global economy in the 2000s, many companies that were part of these industrial complexes went bankrupt after significantly aggravating environmental problems through poor production methods (KICOX, 2008). As a result, the Korean Ministry of Knowledge Economy (MKE) promoted the EIP initiative beginning in 2005 as a way of reducing pollutants while maximizing the efficient use of energy and resources. To date, large industrial complexes have been replaced by EIPs in the South Korean cities of Ulsan, Banwol, Chungju, Yeosu and Pohang. Up to now, these industrial complexes have been emitting much more CO_2 than surrounding areas when per area emission is considered (Fig. 1). However, after converting into EIPs, many waste products produced in these complexes are reused or eliminated through exchange of byproducts and incineration gas utilization, further reducing CO_2 emissions.

In addition to the general use of EIPs in reducing the negative environmental impacts of industry, EIPs can employ efficient technologies to further reduce their, and ultimately the entire country's environmental impact.

The IPAT equation describes the impact of human activity (I) on the environment as a function of population (P), affluence (A) and technology (T) where $I = P \times A \times T$. The IPAT relationship indicates that, among other strategies, effective technological choices can help to reduce a country's environmental impact per unit of economic activity (Song et al., 2011). For example, some environmentally friendly technologies can reduce carbon dioxide emissions by improving CO_2 fixation, utilization, and sequestration (Ahn et al., 2010). One such technological advancement, accelerated mineral carbonation, has recently received attention for its ability to rapidly sequester CO_2, which is especially valuable in countries like South Korea where small land mass limits the amount of CO_2 that can be naturally stored in

geological features (Khoo et al, 2011). EIPs typically use incinerator techniques to burn municipal solid waste products (MSW), which produce a hazardous fly ash that is often too expensive to dispose of with recent landfill taxes (Li et al., 2007). Accelerated mineral carbonation can be used to stabilize solid residues generated from coal-fired power plants as well as other types of combustion residues (e.g. MSW ashes) that make their disposal safer and more cost effective (Rendek et al., 2006).

Although many researchers support the effectiveness of accelerated mineral carbonation of MSW ashes (Li et al., 2007; Ahn et al., 2010; Rendek et al., 2006; Gunning et al., 2010; Montes-Hernandez et al., 2009; Baciocchi et al., 2009; Wang et al., 2010), most carbonation technologies researched in the past used pure CO_2 as the emission being processed despite the fact that the amount of CO_2 in emissions produced through MSW incineration is typically only around 12% (Jiang et al., 2009; Rendek et al., 2006).

In this paper, our objectives are to (1) analyze the characteristics of CO_2 emissions from EIPs and (2) examine the efficacy of accelerated mineral carbonation of gases representative of those actually produced through the incineration of MSW (specifically those containing CO_2).

1 Materials and methods

1.1 Factors decomposition using LMDI analysis

An understanding of the characteristics of CO_2 emissions is critical for controlling and mitigating their release (Zhang et al., 2011). We used the Log Mean Divisia Index (LMDI) method for analysis. This method has previously been recommended for our type of study because of its robust theoretical foundations, strong adaptability, and other desirable properties, including the potential for perfect decomposition. (Ang, 2004, 2005). In addition, the types of data used in this method are readily available, allowing detailed analysis across

time and countries (Zhao et al., 2010).

Under the LMDI approach, the total change in carbon emissions (ΔC_{tot}) through time (0 to T) is the sum of changes in production (ΔC_{pdn}), energy intensity (ΔC_{int}), fuel mix (ΔC_{mix}), emissions (ΔC_{emf}), and population (ΔC_{pop}):

$$\Delta C_{tot} = C^T - C^0 = \Delta C_{pop} + \Delta C_{pdn} + \Delta C_{\text{int}} + \Delta C_{mix} + \Delta C_{emf} \quad (1)$$

where the total carbon emissions (C) for each year *i* and fuel type *j*:

$$C = \sum_{ij} P_i \times \frac{GRDP_i}{P_i} \times \frac{TEC_i}{GRDP_i} \times \frac{EC_{ij}}{TEC_i} \times \frac{CO_{2ij}}{EC_{ij}} = P_i \times G_i \times I_i \times M_{ij} \times E_{ij} \quad (2)$$

in which *P* is population size, *GRDP* is the gross regional domestic product, *TEC* is total energy consumption, and *EC* is fossil fuel energy consumption. In this equation, E_{ij}(calculated as *CO_2/EC*) is the CO_2 emission coefficient arising from fuel *j* in year *i*, M_{ij}(calculated as *EC/TEC*) is the portion of total energy consumption made up of fossil fuel consumption, I_i(calculated as *TEC/GRDP*) is energy intensity, G_i(calculated as *GRDP/P*) is per capita *GRDP*, and P_i is population size. Furthermore, the components of change in Eq. (1) can be calculated as:

$$\Delta C_{pop} = \sum_{ij} L(C_{ij}^T, C_{ij}^0) \ln(\frac{P_i^T}{P_i^0}) \quad (3)$$

$$\Delta C_{pdn} = \sum_{ij} L(C_{ij}^T, C_{ij}^0) \ln(\frac{G_i^T}{G_i^0}) \quad (4)$$

$$\Delta C_{\text{int}} = \sum_{ij} L(C_{ij}^T, C_{ij}^0) \ln(\frac{I_i^T}{I_i^0}) \quad (5)$$

$$\Delta C_{mix} = \sum_{ij} L(C_{ij}^T, C_{ij}^0) \ln(\frac{M_{ij}^T}{M_{ij}^0}) \quad (6)$$

$$\Delta C_{emf} = \sum_{ij} L(C_{ij}^T, C_{ij}^0) \ln(\frac{E_{ij}^T}{E_{ij}^0}) \quad (7)$$

where,

$$L(C_{ij}^{T}, C_{ij}^{0}) = \frac{C_{ij}^{T} - C_{ij}^{0}}{\ln C_{ij}^{T} - \ln C_{ij}^{0}} \quad (8)$$

Here, the CO_2 emission effect (C_{emf}) is the proportion of CO_2 emissions produced through energy conversion or technology development within the same energy source group (e.g. the conversion of light oil into gasoline). The fuel mix effect (C_{mix}) indicates the proportion of CO_2 emissions produced through conversion of energy into other energy source groups (e.g. conversion of coal into natural gas). Finally, the energy intensity effect (C_{int}), production effect (C_{pdn}), and population effect (C_{pop}) represent energy consumption per *GRDP*, per *GRDP* per capita and per change of population, respectively. When these effect coefficients are positive, then a net increase in emissions has occurred, whereas a negative value reflects a net reduction in emissions. Using the decomposition components defined in Eq. (2), we can determine the total change in CO_2 emissions for the EIPs during the period 2006-2009.

On the other hand, we investigated each EIP's characteristic using both period-wise and a time series analysis. Generally, decomposition analysis has an advantage of less data intensive, since a base year and a target year can be only used for a period-wise analysis. However, if index value has a big discontinuity, it can be a grave error with respect to interpretation (Hatzigeorgiou et al., 2008). Thus, we present not only period-wise analysis but also all intervening years through a time series analysis to reduce errors.

1.2 Carbonation mechanism

Carbonation is an exothermic, diffusion-controlling reaction in which the outside surface of a solid is carbonated by the diffusion of CO_2 into its inner region, and the amount of carbonated area becomes larger through time (Bin Shafique et al., 1998; Ahn et al., 2010). The chemical transformation from CaO, $Ca(OH)_2$, and CaClOH to $CaCO_3$ with CO_2 reaction

are shown in Eqs. (9)-(10).

$$CaO + H_2O \rightarrow Ca(OH)_2 + CO_2 \rightarrow CaCO_3 + H_2O \quad (9)$$

$$2CaOHCl + CO_2 \rightarrow CaCO_3 + CaCl_2 + H_2O \quad (10)$$

$$CaCl_2 + 2NH_4OH + H_2O + CO_2 \rightarrow CaCO_3 + 2NH_4Cl + 2H_2O \quad (11)$$

In addition, the carbonation mechanism can be considered a sequential reaction expressed by the following equations (Freyssinet et al., 2002; Li et al., 2007):

$$CO_2(g) \leftrightarrow CO_2(aq) \quad (12)$$

$$CO_2(aq) + H_2O \rightarrow H_2CO_3 \quad (13)$$

$$H_2CO_3 \rightarrow H^+ + HCO_3^- \rightarrow 2H^+ + CO_3^{2-} \quad (14)$$

$$Ca^{2+} + CO_3^{2-} \leftrightarrow CaCO_3 \quad (15)$$

Eq. (12) indicates equilibrium at the gas/liquid interface for dissolution of CO_2 gas. Dissolved CO_2 is converted into carbonate ions according to equilibriums shown in Eqs. (13)-(14). Eventually CO_3^{2-} ions react with Ca^{2+} ions to form $CaCO_3$ as shown in Eq. (15).

We added an additional step to the chain of reactions by creating $CaCO_3$ from $CaCl_2$, as shown in the Eq. (10). When calcium chloride ($CaCl_2$) reacts with water, it dissolves and neutralizes the water's pH (about 8.4). However, in carbonation, an aqueous solution containing calcium chloride should be made more alkaline. Here, we used ammonia as the additive (Eq. 11) so that it would react with H_2CO_3 to form $CaCO_3$.

1.3 Experiment and analysis

To analyze the effectiveness of accelerated mineral carbonation, we sampled fly ash from the bag house section of a waste incinerator. The main elements in this ash were calcium and chloride (Table 1). We divided the ash into three parts: (1) a raw, untreated control sample, (2) a carbonation treatment sample with no ammonia additives, and (3) a second carbonation

treatment sample with ammonia added. We noted the amount of time it took for the pH of the carbonation treatment samples to change. We also noted the mineralogy, morphology, and microstructure as well as reaction times, pH changes, and CO_2 gas inflow speeds for the treated and untreated samples.

Before carbonation, the raw sample was dried at 105°C for 24 h and reweighed. Thereafter, 10g of each sample was suspended in 300ml of deionized water at room temperature and treated with mixed gas (1:9, CO_2: N_2) in a gas diffuser (Fig. 2). A micro-bubble generator was utilized AURA TEC (OM4-MDG-020). We then divided the mixture into two parts: (1) CO_2 0.5 L/min, N_2 4.5 L/min and (2) CO_2 0.1 L/min, N_2 0.9 L/min to investigate inflow speed. We also measured the weight gain of the ash as a result of this reaction in triplicate and used mean value.

We performed thermo-gravimetric and differential thermal analysis (TG/DTA) on ashes using a Thermo plus EVO TG 8120 thermo analyzer in a temperature range of ambient-1000°C at a heating rate of 10°C/min and noted the weight changes through time. The area between 550°C and 850°C of the resulting TG curve, where the slope represents the change in mass and decomposition rate, was used to determine the CO_2 content of the sample because mass change in this region of the curve is assumed to be attributable to the release of CO_2 through $CaCO_3$ decomposition (Ahn et al., 2010). Eventually, through TG/DTA analysis, CO_2 uptake efficiency by weight loss can be calculated like Eq. (16).

CO_2 uptake efficiency (%):

$$(\alpha_1 - \beta + \alpha_2) / \gamma \times 100 \quad (16)$$

where, α_1 is first step carbonated weight, β, carbonated raw material weight, α_2, second step carbonated weight, and γ, CO_2 conversion volume to $CaCO_3$.

We also determined the mineral phases of the ashes through X-ray powder diffraction

with Cu Kα radiation using a RIGAKU (equipped with a copper tube operated at 40kV and 60 Ma) with an angular step of 0.02° held for 2 s with 2θ spanning from 5 to 80°. The microstructures of the raw and carbonated fly ash after CO_2 capture were analyzed using scanning electron microscopy (SEM). The full experimental procedure is shown in Fig. 3.

2 Results and Discussions

2.1 Characteristics of CO_2 emissions from EIPs

Our results showed that the driving force behind increased CO_2 emissions for the five EIPs analyzed (Fig. 1) was related to the production effect but that decreases in the energy intensity effect led to a reduction in carbon emissions, resulting in a net increase/decrease in carbon emissions from the EIPs from 2006 to 2009. (Figs. 4&5).

At the Ulsan EIP, which is South Korea's largest center of ship, automobile, and petrochemical production (KICOX, 2008), the production effect was the main driving force behind the creation of CO_2 emissions. However, the production effect was offset by the energy intensity effect, resulting in an increase of only 0.58MtCO_2 from the 2006 level. Similarly, the Yeosu EIP, which is representative of most industrial complexes in South Korea (KICOX, 2008), had CO_2 emissions attributable to the production effect. However, that effect was also offset by a substantial improvement in the energy intensity effect, resulting in a net emission loss of -1.1MtCO_2 from the 2006 level.

The Banwol EIP, which is in close proximity to the capital city, is easily accessible from almost everywhere in the country because of the metropolitan transportation system (KICOX, 2008). However, probably because it is composed of small and medium companies, this EIP showed few or no improvement in terms of processes and technologies that would reduce CO_2 emissions, although most factors acted as the decrease of CO_2 emissions.

The Chungju EIP is composed of the electronic & electric industries that produce, for example, display and semiconductor parts as well as next generation and solar batteries (KICOX, 2008). Here, the production effect led to an increase in CO_2 emissions while the energy intensity and population effects did not cause a remarkable decrease in emissions.

Finally, the Pohang EIP, which is home to a variety of manufacturing industries (e.g. metal, ceramic, electronic & electric, and chemical), showed increased emissions as a result of the production effect and decreased emissions through the energy intensity and population effects. The population effect was the main contributor to the decline in carbon emissions, although this trend is likely to change as the result of reorganizing of administrative districts in 2008.

2.2 Accelerated mineral carbonation

2.2.1 Morphology

MSW fly ash is highly alkaline due to the existence of $Ca(OH)_2$, and CaO, which is detrimental to its reuse. The raw fly ash was a gray powdery material that became darker and harder with the first carbonation step and finally white and powdery with the second carbonation step following the addition of ammonia (Fig. 6). After all, in our study, carbonated ashes can be used various fields. Gray carbonated fly ash can be utilized as aggregates in the concrete industry and white products can be used as filler in the paper-making industry.

2.2.2 Effect of pH: bubbling and micro-bubbling for carbonation

The pH of samples changed over time in response to carbonation reactions (Fig. 7). In general, the initial pH by samples was between 12 and 13 and fell to between 10 and 7 during carbonation (Li et al., 2007; Wang et al., 2010). We assumed when pH of the suspension became less than 7, at which point the carbonation was completed (Ahn et al., 2010). The aim

is to find the optimal condition for efficient accelerated mineral carbonation.

With high flow inlet gas techniques, it took about 5 min with micro-bubbling and about 9 min with bubbling for carbonation to occur for samples not containing the ammonia additive. Using low flow inlet gas techniques, carbonation completion times were about 4min (micro-bubbling) and about 8 min (bubbling) for samples not containing the ammonia additive. Thus, micro-bubbling carbonation with low flow inlet gas was the optimal condition for efficient accelerated mineral carbonation in our study.

2.2.3 CO_2 uptake efficiency

Considering our raw sample, we found that mass changed by 7.14% with carbonation, indicating the raw fly ash contained about 0.7g of $CaCO_3$. The presence of calcite in the original fly ash may have been caused by earlier partial weathering of the ash (Wang et al., 2010).

In addition, during the first carbonation step before ammonia has been added to the system, we determined varying carbonation efficiency through time (Fig. 8). At 4 min into the carbonation, CO_2 uptake efficiency was 33.93% (pH 7.2) and gradually decreased to 18.13%, 10.06% and 6.22% for 5 min, 10min and 15min, respectively. Because the pH fell below 7 after 4 min, we knew that the carbonation reaction ended at this time, which explains the drastic reduction in the CO_2 uptake after this point. On the other hand, at 3 min into the carbonation, pH was 11.67. Thus, we established that the first carbonation step was complete at 4 min.

In the second carbonation step, where we added ammonia into an aqueous solution after first step carbonation, to increase pH levels, CO_2 uptake efficiency increased up to a moderate concentration of ammonia (Fig. 9).

When pH was increased to 10 (ammonia: 0.03 mol/L) and carbonation for 5 min, CO_2 uptake

efficiency was 19.90% and further increased to 25.32% at a pH of 10.5 (ammonia 0.06 mol/L). However, efficiency declined to 20.80% at a pH of 11(ammonia 0.16 mol/L), to 17.08% at a pH of 11.5 (ammonia 0.32 mol/L), and 14.65% at a pH of 12(ammonia 1.65 mol/L). We can recognize that ammonia is necessary to promote the reaction of CO_2, but too much ammonia limits the reaction. Thus, we determined that carbonation was most effective for carbon sequestration at a pH up to 10.5.

Under an initial pH of 10.5 in the second step where carbonation is most effective, we also found that carbonation was still at its most efficient up to the first 3 min of the reaction (Fig. 10). At 3 min into the carbonation reaction, CO_2 uptake efficiency was 58.63% (pH 8.32) but declined to 21.53% (pH 7.02) after 4 min and to 17.09% (pH 6.95) after 5 min. On the other hand, at 2 min into the carbonation reaction, CO_2 uptake efficiency was 49.52% (pH 9.23).

Finally, The efficiency of $CaCO_3$ production from Ca conversion within the first 4 min of the carbonation reaction, however, substantially improved with the ammonia additive; $CaCO_3$ production was at 24.65% in the first step (no ammonia) but increased to 56.59% in the second step of reaction (with ammonia additive).

2.2.4 Mineral phases in fly ash

We determined that the carbonated fly ash sample was composed of a mixture of predominantly Ca-rich compounds compared to the raw fly ash sample which contained compounds rich in chloride (e.g. NaCl and CaClOH; Fig. 11). The most obvious differences were an increase in calcite peak intensity and a decrease in CaClOH and $Ca(OH)_2$ compounds in the carbonated sample compared to the original raw sample. In addition, a peak in $CaSO_4$ occurred in the carbonated sample without ammonia but disappeared after addition of the ammonia additive.

2.2.5 Microstructure

SEM images revealed distinct differences in the morphology of the original, carbonated without ammonia, and carbonated with ammonia fly ash samples (Fig. 12). The original sample had a granular, rough appearance with individual grains clearly visible (Fig. 12a). The carbonated ash without the ammonia appeared to have newly precipitated calcites, but a crystal is not clear, and also particles became more compact with gypsum inter-mixed (Fig. 12b). Carbonated ash with the ammonia contained larger, more clearly visible calcite molecules. It is demonstrative that carbonation is a diffusion-controlling reaction in which the outside surface of a solid is carbonated by the diffusion of CO_2 into its inner region, and the amount of carbonated area becomes larger through time (Fig. 12c,d,e,f).

3 Conclusions

EIPs and the technologies they employ can play an important role in the reduction of CO_2 emissions thought to contribute to global climate change. In this study, we investigated trends in CO_2 emission production as well as the efficacy of accelerated mineral carbonation techniques used at five EIPs in South Korea. Using decomposition analysis, we found that the production effect was the main contributor of carbon emissions at the EIPs but also that a decline in the energy intensity effect mitigated carbon emission production in all EIPs. In addition, fuel mix and population effects led to insignificant reductions in emissions.

In our analysis of the efficacy of accelerated mineral carbonation, we found that ammonia was an important addition in the simplified two-step carbonation reaction we proposed. We also found that micro-bubbling and gas inflow speed had a major influence on reactions. CO_2 uptake efficiency was 33.93% in the first step of the carbonation process and 58.63% in the second step. $CaCO_3$ as a product of Ca conversion was obtained up to a

maximum of 56.59% through first and second carbonations. Mineralogical analysis of ash by XRD showed a disappearance of $Ca(OH)_2$ and CaClOH as well as an increase in the amount of $CaCO_3$ following accelerated carbonation. Finally, SEM analysis also revealed that the fly ash particles became more crystalline with agglomeration following carbonation with ammonia.

Consequently, we can apply our findings in the EIPs as shown in Fig. 13. There are many incinerators for incineration of waste materials generated in the EIPs. These ashes produced from the incinerators can be collected in the accelerated mineral carbonation plant, and then be treated dividing into two steps. The product from the first step carbonation can be utilized with manifold purposes such as mine restoration, reuse in construction and disposal. The product from the second step carbonation can be used paper manufacture as a high value product because of its color. Furthermore, remaining aqueous solutions after first and second step carbonation can be reused for the first step carbonation. That is, the water used in the first step carbonation is to be circulated in this process steadily. Fig. 14 is the proposed network to be implemented with the existing network in the Ulsan EIP. For example, the incinerators of the Yoosung corp. incinerate about 95 ton/d of industrial waste. The Sungam municipal waste incineration facility (MWIF) also has two incinerators, each with an incineration capacity of 320 ton/d. To date, some companies in this EIP manufactured synthesis zeolite using fly ashes produced from incineration facilities, and disposed of heavy metals within wastewater. However, we can use fly ash in various ways by applying our findings. Dau Metal in Ulsan EIP is generated wastewater containing high-enriched ammonia. This company converted it into a nutrient (ammonium phosphate), and then this nutrient (30 ton/d) was utilized by the microbes during wastewater treatment in Taekwang industry up to now. However, a portion of wastewater containing high-enriched ammonia can be supplied to

the accelerated mineral carbonation plant we propose. It is estimated that recycling rate will be increasing significantly.

Acknowledgements

The authors were supported by the Global COE Program, “Global Center of Excellence for Mechanical Systems Innovation” and by the Ministry of Education, Science, Sports and Culture, Grant-in-Aid for Scientific Research (A). We are deeply obliged to these organizations.

References

Ang B W, 2004. Decomposition analysis for policymaking in energy: which is the preferred method? Energy Policy, 32(9):1131-1139.

Ang B W, 2005. The LMDI approach to decomposition analysis: a practical guide. Energy Policy, 33(77):867-871.

Ahn J W, Lim M H, Han G C, You K S, 2010. Environmental Remediation and Conversion of Carbon Dioxide (CO_2) into Useful Green Products by Accelerated Carbonation Technology. Environmental Research and Public Health, 7: 203-228.

Baas L W, Boons F A, 2004. An industrial ecology project in practice: exploring the boundaries of decision-making levels in regional industrial systems. Journal of Cleaner Production 12 (8-10): 1073-1085.

Baciocchi R, Costa G, Polettini A, Pomi R, Prigiobbe V, 2009. Comparison of different reaction routes for carbonation of APC residues. Energy Procedia, 1: 4851-4858.

Baciocchi R, Costa G, Bartolomeo E D, Polettini A, Pomi R, 2009. The effects of accelerated carbonation on CO_2 uptake and metal release from incineration APC residues. Waste Management, 29: 2994-3003.

Berkel R V, Fujita T, Hashimoto S, Geng Y, 2009. Industrial and urban symbiosis in Japan: Analysis of the Eco-Town program 1997-2006. Journal of Environmental Management, 90(3): 1544-1557.

Bin Shhafique S, Walton J, Gutierrez N, Smith R, Tarquin A, 1998. Influence of carbonation on leaching of cementitious waste forms. Environmental Engineering, 22: 463-467.

Fang Y, Cote R P, Qin R, 2007. Industrial sustainability in China: Practice and prospects for eco-industrial development. Journal of Environmental Management, 83 (3): 315-329.

Freyssinet P h, Piantone P, Azaroual M, Itard Y, Clozel-Leloup B, Gyuonnet D, Baubron J C, 2002. Chemical changes and leachate mass balance of municipal solid waste bottom ash submitted to weathering. Waste Management, 22: 159-172.

Gibbs D, Deutz P, 2005. Implementing industrial ecology? Planning for eco-industrial parks in the USA. Geoforum, 36: 452-464.

Gibbs D, Deutz P, 2007. Reflections on implementing industrial ecology through eco-industrial park development. Journal of Cleaner Production, 15(17): 1683-1695.

Gunning, P J, Hills C D, Carey P J, 2010. Accelerated carbonation treatment of industrial wastes. Waste Management, 30: 1081-1090.

Hatzigeorgiou E, Polatidis H, Haralambopoulos D, 2008. CO_2 emissions in Greece for 1990-2002: A decomposition analysis and comparison of results using the Arithmetic Mean Divisia Index and Logarithmic Mean Divisia Index techniques. Energy, 33(3):492-499.

Intergovernmental Panel on Climate Change (IPCC), 2007. IPCC guidelines for national greenhouse gas inventories. Available at: http://www.ipcc.ch/ publications _ and_data/ ar4/syr/en/spm.html.

International Energy Agency (IEA), 2011. CO_2 emissions from fuel combustion Highlights. Available at: http://www. Iea.org/about/copyright.asp.

Jiang J G, Du X J, Chen M Z, Zhang C, 2009. Continuous CO_2 capture and MSWI fly ash stabilization, utilizing novel dynamic equipment. Environmental Pollution,

157: 2933-2938.

Khoo H H, Bu J, Wong R L, Kuan S Y, Sharratt P N, 2011. Carbon capture and utilization: preliminary life cycle CO_2, energy, and cost results of potential mineral carbonation. Energy Procedia, 4: 2494-2501.

Korea Industrial Complex Corporation (KICOX), 2008. Outlook of industrial complexes in Korea. Report.

Li X, Bertos M F, Hills C D, Carey P J, Simon S, 2007. Accelerated carbonation of municipal solid waste incineration fly ashes. Waste Management, 27: 1200-1206.

Montes-Hernandez G, Perez-Lopez R, Renard F, Nieto J M, Charlet L, 2009. Mineral sequestration of CO_2 by aqueous carbonation of coal combustion fly-ash. Hazardous Materials, 161: 1347-1354.

Presidential Committee on Green Growth (PCGG), 2009. Greenhouse gas reduction goals of major countries and recent changes in circumstances. Available at: http://www. greengrowth.go.kr.

President's Council on Sustainable Development (PCSD), 1996. In: Eco-industrial park workshop proceedings. Washington (DC).

Rendek E, Ducom G, Germain P, 2006. Carbon dioxide sequestration in municipal solid waste incinerator (MSWI) bottom ash. Hazardous Materials, B128: 73-79.

Roberts B H, 2004. The application of industrial ecology principles and planning guidelines for the development of eco-industrial parks: an Australian case study. Journal of Cleaner Production 12, 997-1010.

Song M, Wang S, Yu H, Wu J, 2011. To reduce energy consumption and to maintain rapid economic growth: Analysis of the condition in China based on expended

IPAT model. Renewable and Sustainable Energy Reviews, 15(9):5129-5134.

Tudor T, Adam E, Bates M, 2007. Drivers and limitations for the successful development and functioning of EIPs (eco-industrial parks): A literature review. Journal of Ecological Economics 61: 199-207.

Wang L, Jin Y, Nie Y, 2010. Investigation of accelerated and natural carbonation of MSWI fly ash with a high content of Ca. Hazardous Materials, 174: 334-343.

Zhang L, Yuan Z, Bi J, Zhang B, Liu B, 2010. Eco-industrial parks: national pilot practices in China. Journal of Cleaner Production, 18 (5): 504-510.

Zhang Y, Zhang J, Yang Z, Li S, 2011. Regional differences in the factors that influence China's energy-related carbon emissions, and potential mitigation strategies. Energy Policy, 39(12):7712-7718.

Zhao M, Tan L, Zhang W, Ji M, Liu Y, Yu L, 2010. Decomposing the influencing factors of industrial carbon emissions in Shanghai using the LMDI method. Energy, 35(6):2505-2510.

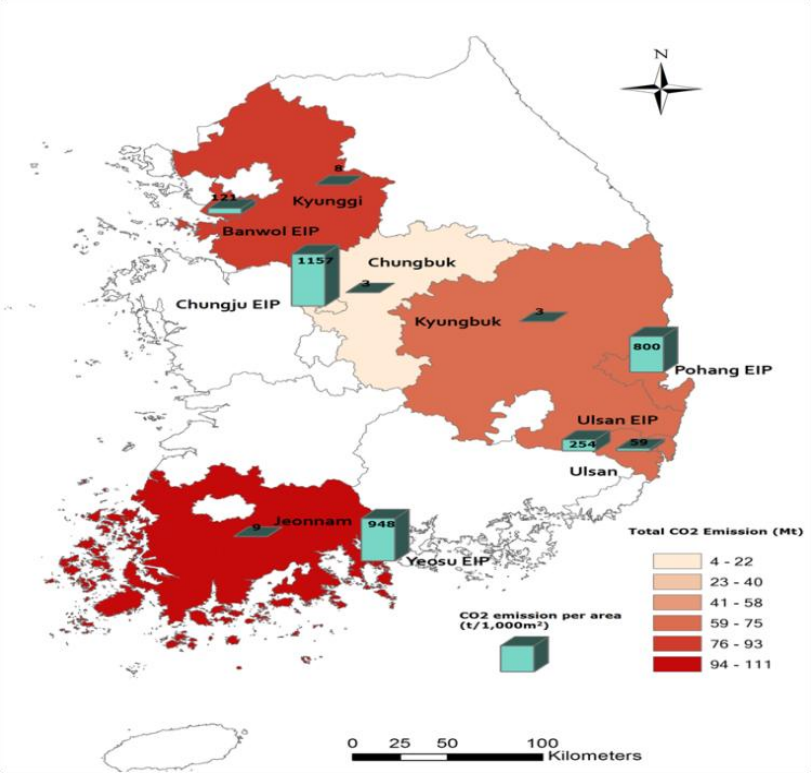

Fig. 1. Total CO_2 emission and emission per area in five regions and EIPs

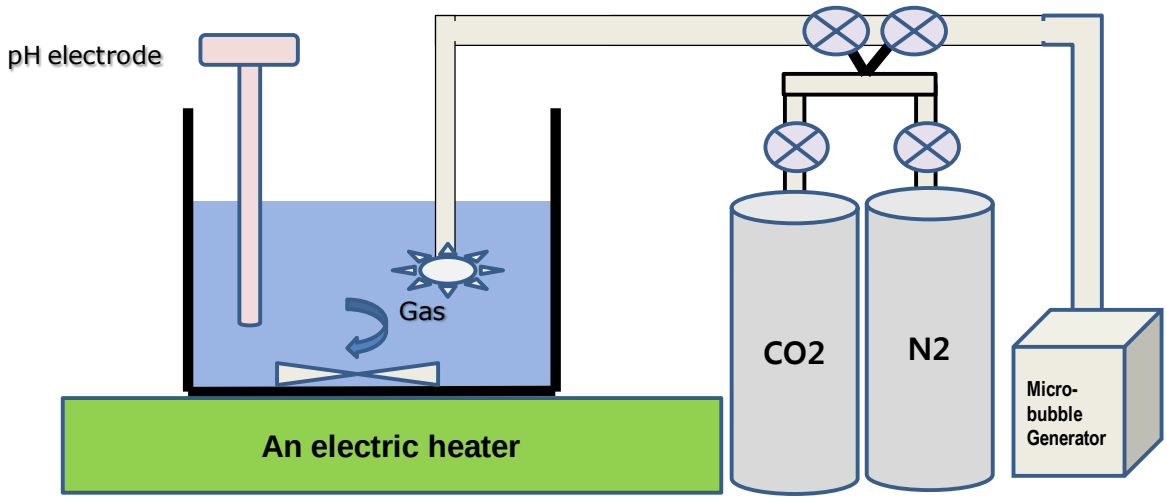

Fig. 2. Apparatus for accelerated mineral carbonation of fly ash

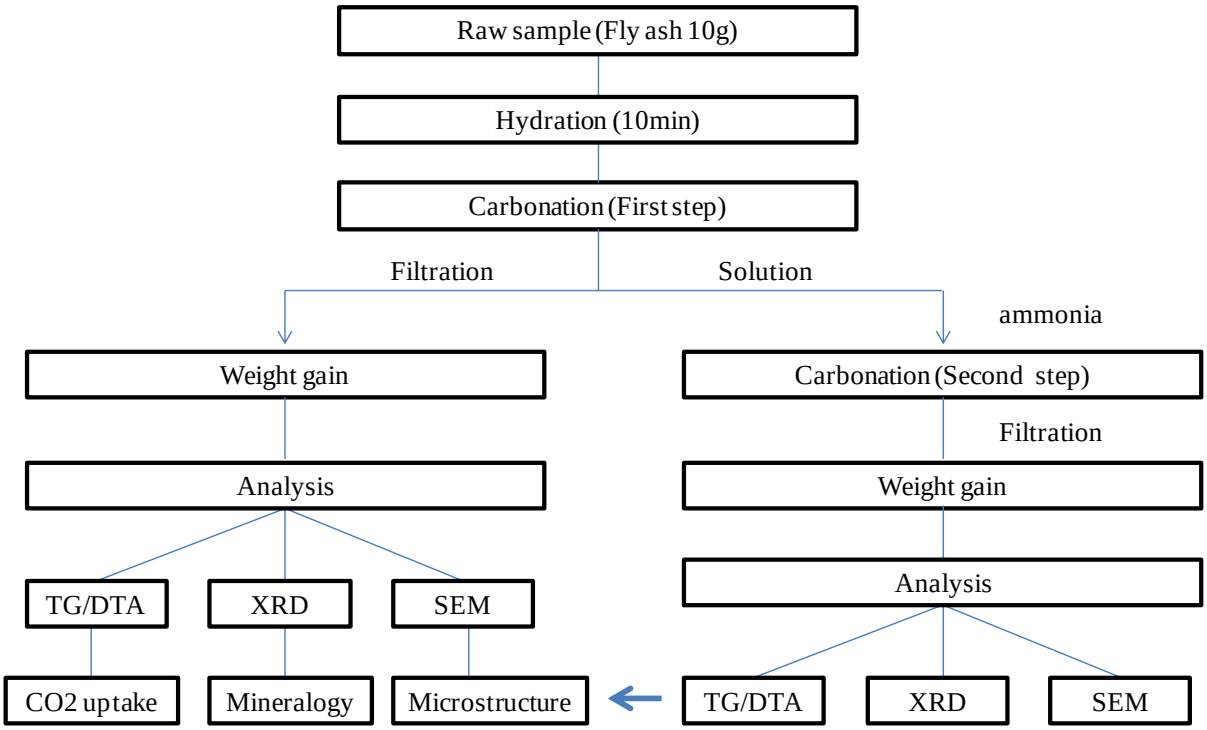

Fig. 3. Experiment procedure flow chart

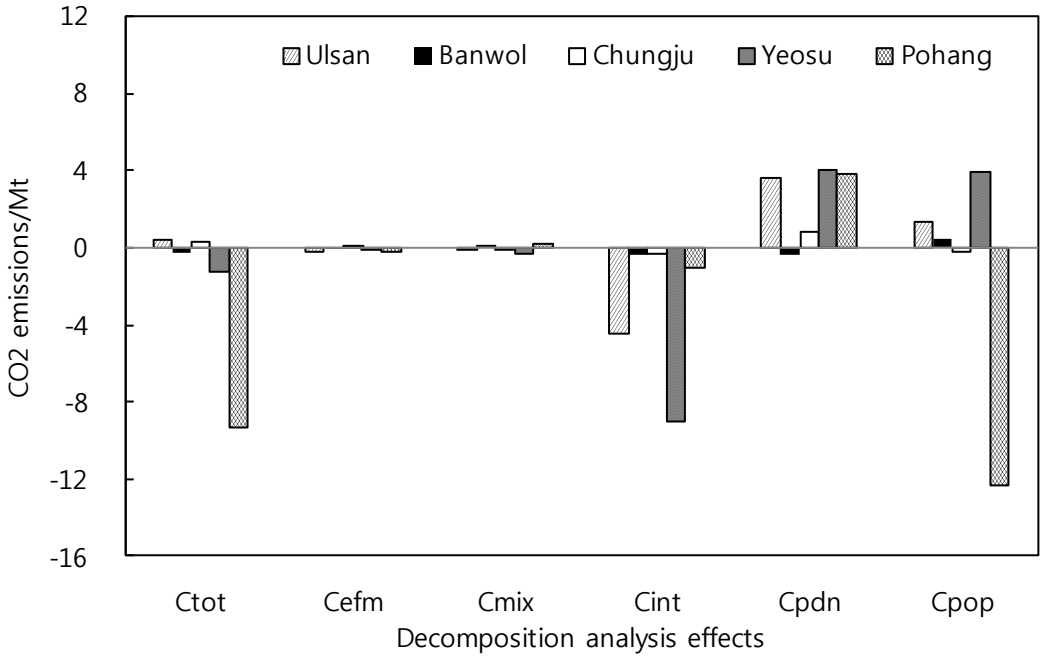

Fig. 4. Factors causing the CO_2 emission between 2006 and 2009 in South Korea's EIPs

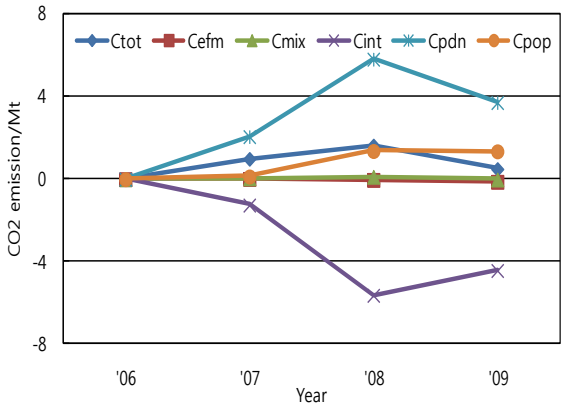

<Ulsan EIP>

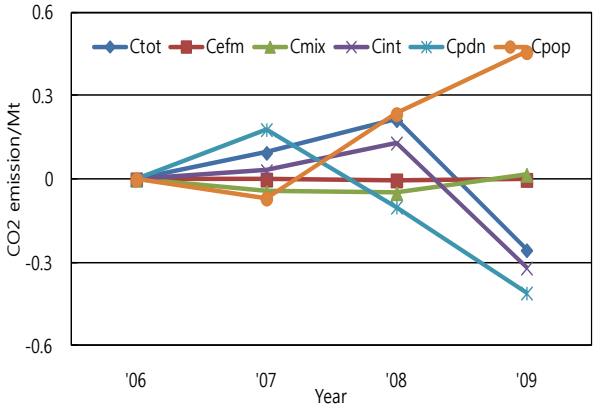

<Banwol EIP>

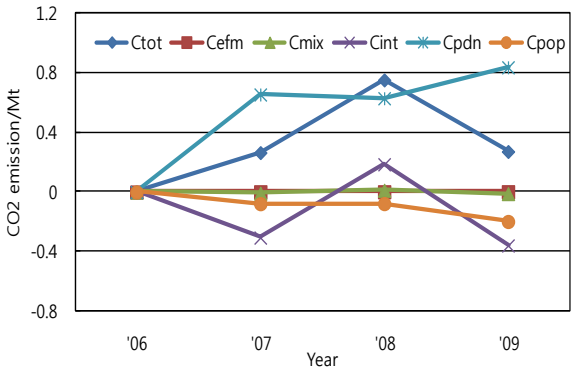

<Chungju EIP>

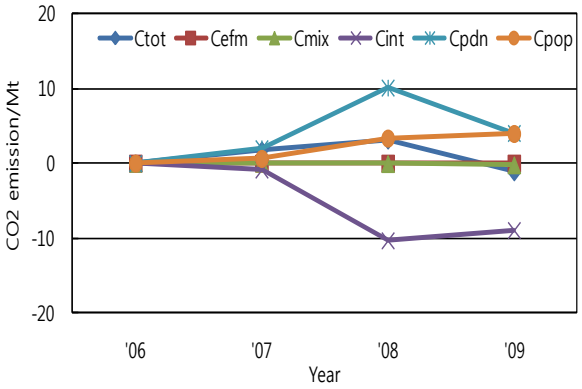

<Yeosu EIP>

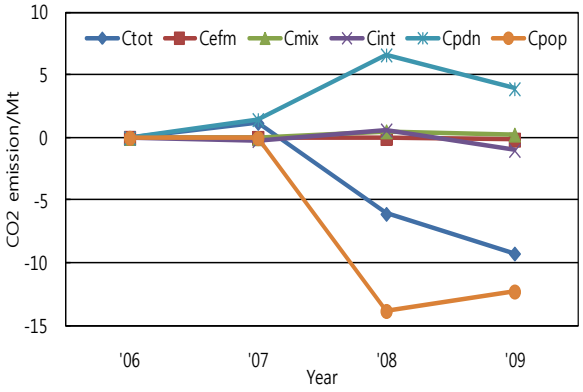

<Pohang EIP>

Fig.5. Factors causing the CO_2 emission in each EIP by a time series.

< Raw fly ash > < 1st step carbonation > < 2nd step carbonation >

Fig. 6. Phased sample morphology

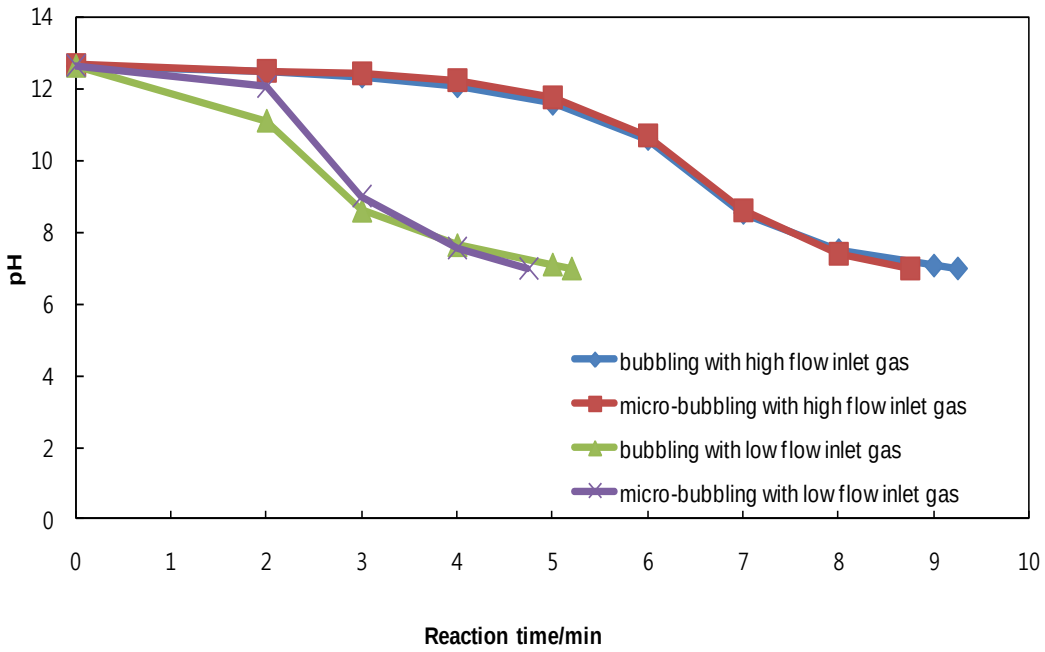

Fig. 7. pH change between high flow inlet gas (CO_2:N_2, 0.5 L/min:4.5 L/min) and low flow inlet gas (CO_2:N_2, 0.1 L/min:0.9 L/min)

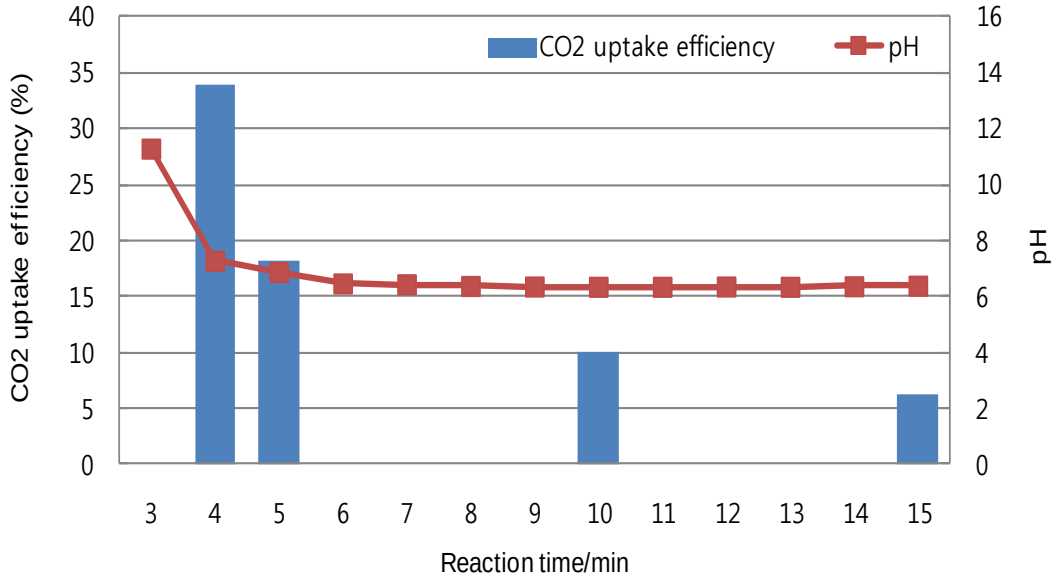

Fig. 8. CO_2 uptake efficiency in the first step carbonation

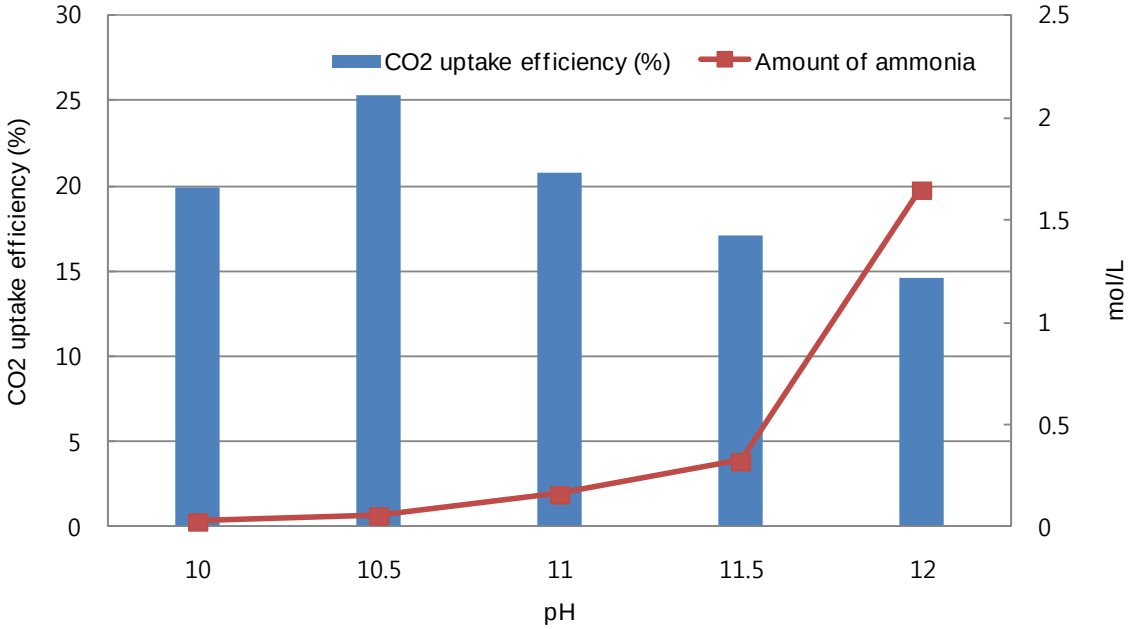

Fig. 9. CO_2 uptake efficiency by change of pH in the second step 5min carbonation

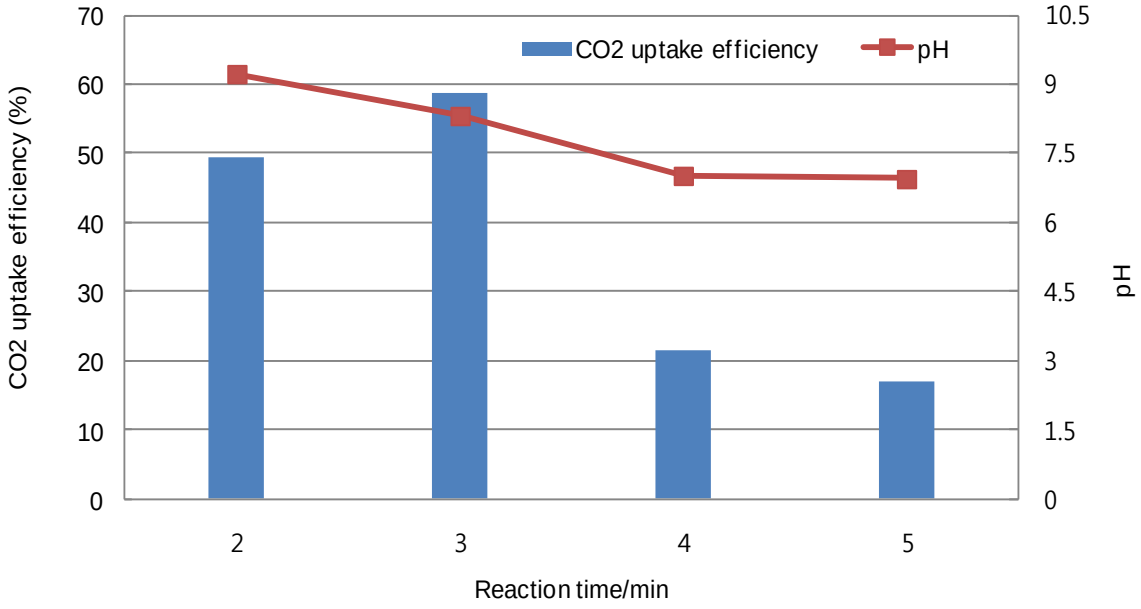

Fig. 10. CO_2 uptake efficiency by time in the second carbonation

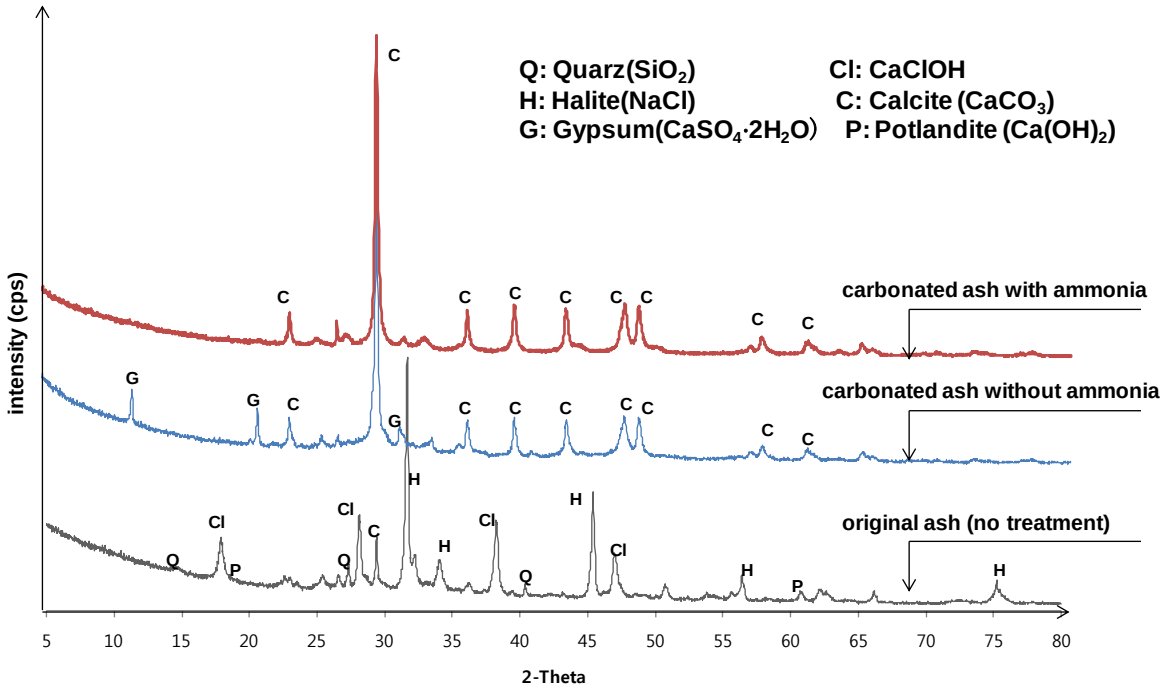

Fig. 11. XRD patterns of original and carbonated fly ash

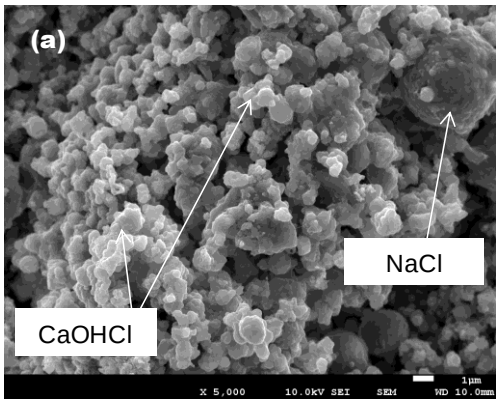

Raw ash (×5,000)

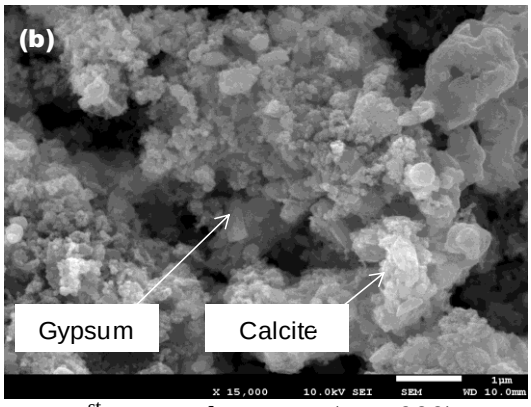

1st step carbonation (×15,000)

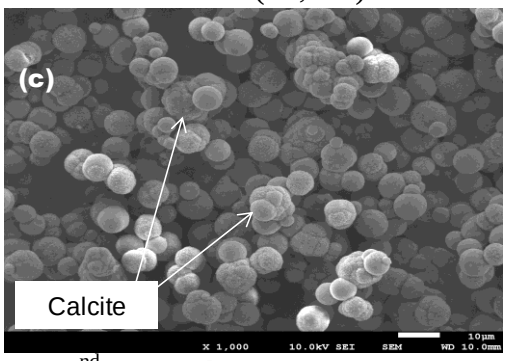

2nd step carbonation (×1,000)

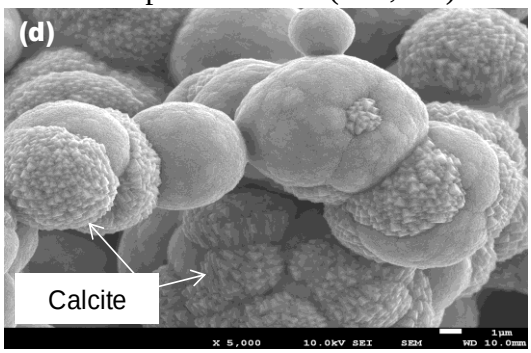

2nd step carbonation (×5,000)

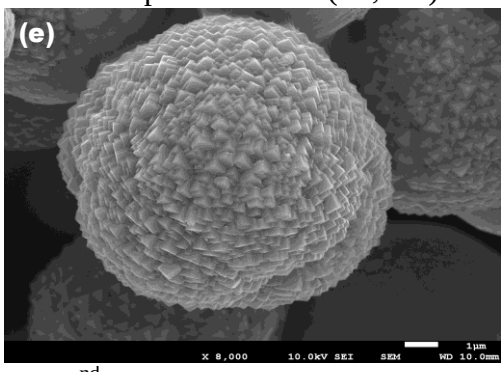

2nd step carbonation (×8,000)

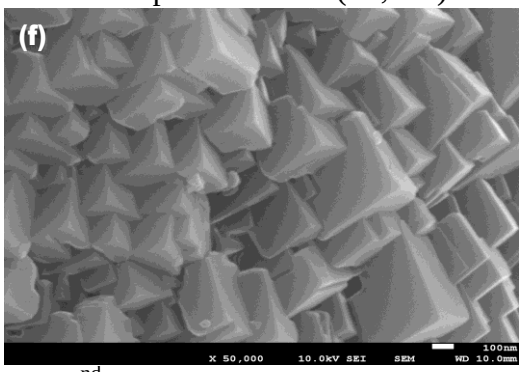

2nd step carbonation (×50,000)

Fig. 12. Microstructure of the raw and carbonated fly ash

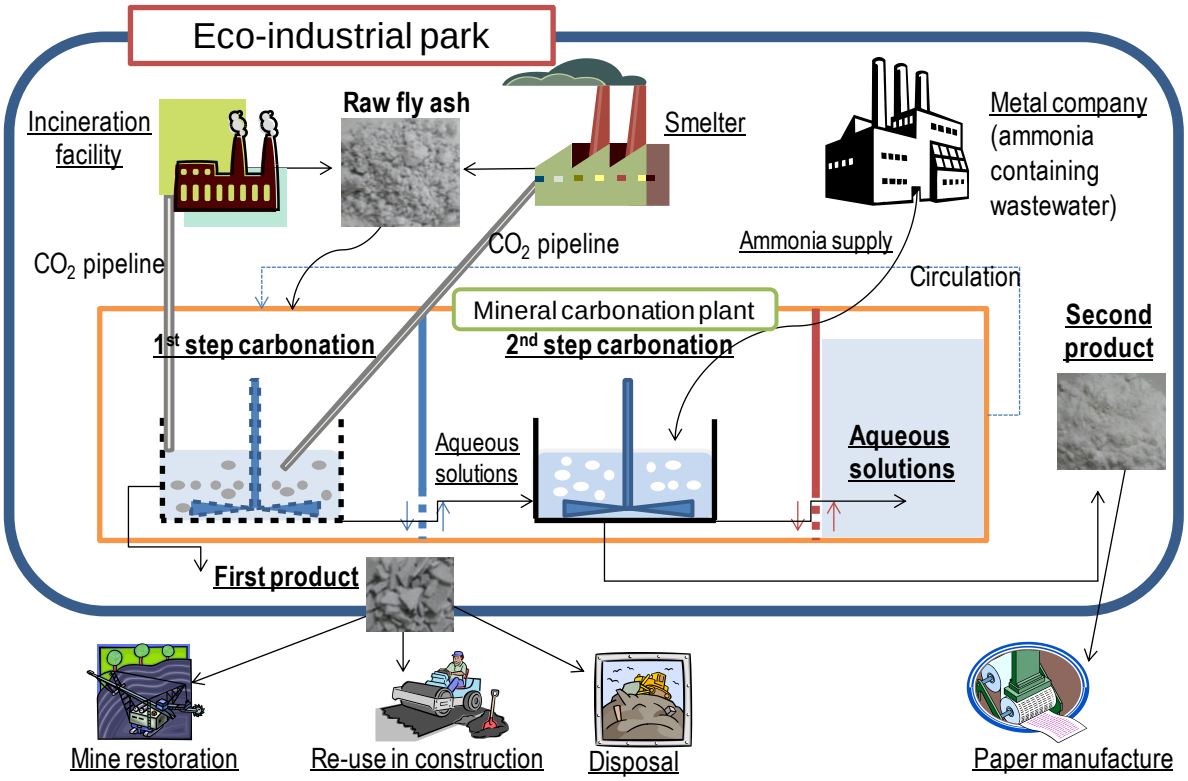

Fig. 13. Material fluxes and process associated with the two-step carbonation in the EIPs

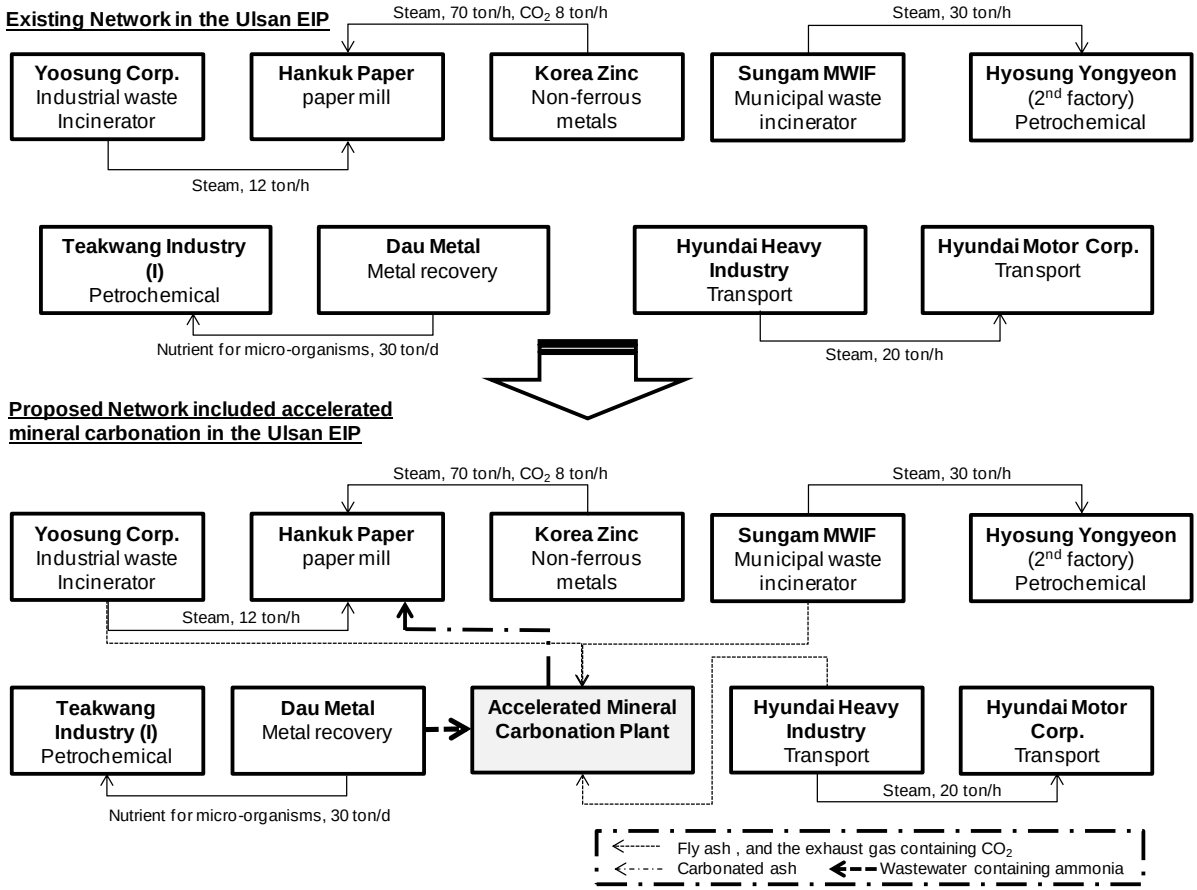

Fig. 14. Existing network and proposed network included accelerated mineral carbonation in the Ulsan EIP

Table 1
Main elements analysis of the fly ash

Elements	wt.%	Elements	wt.%	Elements	wt.%
F	1.08	S	4.70	Ni	0.04
Na	10.82	Cl	26.45	Fe	0.33
Cr	0.03	K	1.65	Pb	0.26
Al	0.12	Ca	30.42	Cu	0.19
Si	0.31	Ti	0.09	Zn	1.56
P	0.97	Mn	0.05	Br	2.79